Journal of Energy Storage 33 (2021) 101926

Contents lists available at ScienceDirect

Journal of Energy Storage

journal homepage: www.elsevier.com/locate/est

New phase change material storage concept including metal wool as heat transfer enhancement method for solar heat use in industry

Cristina Prieto[a,b,*], Carlos Rubio[a], Luisa F. Cabeza[c]

[a] Abengoa Energia, c/ Energía Solar 1, 41012 Sevilla, Spain
[b] University of Seville, Department of Energy Engineering, Camino de los Descubrimientos s/n, 41092, Seville, Spain
[c] GREiA Research Group, INSPIRES Research Centre, Universitat de Lleida, Pere de Cabrera s/n, 25001 Lleida, Spain

ARTICLE INFO

Keywords:
Latent heat storage
Phase change material
Thermal conductivity enhancement technique
Metal wool

ABSTRACT

Thermal energy storage is recognized as a key technology in the energy transition the world is facing today. But the main technical barrier this technology has to achieve wider deployment the low thermal conductivity of the materials used, the so-called phase change materials (PCM). This paper presents a new concept for thermal conductivity enhancement of a PCM tank using metal wool. Metal wool is one of the least studied method to enhance PCM thermal conductivity, while it has high potential to do so at a low cost. This study shows the experimental prototype that developed for the validation of the effective conductivity of the composite formed by $NaNO_3$ salts and metal wool. The metal wool used is produced and arranged to ensure the right porosity and packaging to increase 300% the effective thermal conductivity of the mixture. The model validated confirms the movement of the fluid during the melting standardizes the temperature of the molten material, increasing the transference. The model also validates the new composite, with wool and $NaNO_3$ as PCM, as one of the most promising materials to be used in applications that need heat to be stored at around 280–300 °C. Such applications include use of solar energy and waste heat in industry.

1. Introduction

The use of phase change materials (PCM) to store solar energy in different applications was developed by many researchers in the last two decades, and the use of this technology in the so-called high temperatures applications is increasing [1–4]. Within this context, high temperature applications are those using storage at temperatures higher than 150 °C, going up to 1000 °C in applications such as concentrated solar power, and being between 200 °C and 400 °C in applications that use solar energy in industry or for industrial waste heat recovery.

Nevertheless, most authors coincide that one of the main drawbacks for the use of PCM when high power is needed is the low thermal conductivity of the materials. Gasia et al. 2016 [5] shows a detailed review of the thermal conductivity enhancement techniques found in the literature. These techniques were classified as the addition of extended surfaces (fins or heat pipes) or the combination of highly conductive materials with the PCM (such as graphite, metal foams, or nano-additives).

Although fins are commonly used in the industry, the transient behaviour of PCM heat exchange add up other challenges to be considered, such as the shape and position of the fins [6]. The use of graphite foams with high porosity is the other highly; here the main challenge is the infiltration of the PCM in the graphite matrix. When highly conductive particles are added in the PCM the main drawback is the deposition of the particles after several thermal cycles.

A comparison of the different techniques, with their main advantages and drawbacks are presented in Table 1. The properties considered for the comparison were technical ones (high thermal conductivity enhancement, easy optimization of the storage system, and easy inclusion of the PCM), economical (low cost), of system performance (control of the PCM volume expansion and potential corrosion), and environmental (waste/by-product and easy disposal after use). Metal fins and graphite composite are ticked as positive in only three of those aspects, while metal fibres have more positive aspects than negative ones.

Badenhorst 2019 [7] recently presented a deep review of the application of carbon materials in PCM systems. It is interesting to see that thermal conductivity enhancement was much higher in continuous composites and matrix than in particulate additives (graphite foams k = 30–270 W/m•K vs. graphitic fibres k = 0.3–8.0 W/m•K).

One of the less explored thermal conductivity enhancement techniques is the use of metal wool, while its potential for high thermal

* Corresponding author.
E-mail address: cristina.prieto@abengoa.com (C. Prieto).

https://doi.org/10.1016/j.est.2020.101926
Received 23 October 2019; Received in revised form 17 September 2020; Accepted 20 September 2020
Available online 01 October 2020
2352-152X/

Table 1
Comparison of thermal conductivity enhancement techniques.

Advantage	Metal fins	Metal fibres	Nano-additives	Graphite composite
High thermal conductivity enhancement	✓	✗	✓	✓
Easy optimization of the system	✗	✓	✗	✗
Easy inclusion of the PCM	✓	✓	✓	✗
Low cost	✓	✓	✗	✗
Control of the PCM volume expansion	✗	✗	✗	✗
Potential corrosion	✗	✗	✗	✓
Waste/by-product	✗	✓	✗	✗
Easy disposal	✗	✓	✗	✗

conductivity enhancement with a low cost. This thermal conductivity enhancement technique has shown good potential in low temperature applications [8,9]. Recently, Yousef et al. 2019 [10,11] studied the use of a latent heat storage system in a solar still, using metal wool fibres as heat transfer enhancement method, comparing the performance of the storage system with other heat transfer enhancement methods (such as fins); they measured experimentally an increase of 25% in the daily productivity of fresh water. Nevertheless, this heat transfer enhancement method is one of the least studied. To contribute to this gap in the literature, this paper presents a new concept to use PCM in high temperature applications using metal wool as thermal conductivity enhancement.

2. Materials and method

The metal wool, also called metal matrix, is formed by several fibres with a given orientation, obtained when cutting a metal cable with blades. The fibres have a diameter between 10 and 300 μm and a thermal conductivity of 40 W/m•K. The properties of the fibres are included in Table 2.

The PCM used in $NaNO_3$ from SQM®, refined grade, with the properties shown in Table 3 and Table 4.

The storage tank is to a shell and tube heat exchanger with the heat transfer fluid flowing inside the tube and the PCM in the shell. In the experimental set-up, the heating was carried out with an electrical heater (Fig. 1). The metal wool is placed in the PCM side of the tank with the fibres in 16 layers orientated perpendicular to the inner pipe to ensure best heat transfer; each layer of fibres changes the heat transfer direction (Fig. 2) to avoid the preferential direction. The thermal conductivity coefficient of pure sodium nitrate considered was 0.50 W/m•K, value found in the literature [12]. The porosity of the wools used in the prototype was 98.6%

Table 2
Properties of the metal fibre by Barlesa®.

Property	Value
Material	Stainless steel (AISI 424]
Supplier	Barlesa®
Density [kg/m^3]	199
Pure steel density[kg/m^3]	7800
Porosity [ppu]	0.97
Thermal conductivity aligned [W/m•K]	3
Thermal conductivity normal [W/m•K]	1.1

Table 3
PCM used properties.

Property	$NaNO_3$
Melting enthalpy	177 kJ/kg
Melting temperature	307 °C
Density	2260 kg/m^3
Volume expansion	16%
Cost	0.38 €/kg

Table 4
$NaNO_3$ PCM properties.

Characteristic / Property	Value
Energy density	177 kJ/kg
Specific heat	1.65 kJ/kg•K
Melting point	~305 °C
Thermal conductivity	~0.5 W/m•K

To be able to register the temperature distribution in all the storage tank, 24 thermocouples of contact, model TE 67.50 (max. operating temperature 400 °C, type K, limiting error ± 1.5 °C), supplied by Wika® were inserted as shown in Fig. 3 (12 internal thermocouples for monitoring internal temperature, 12 surface thermocouples for monitoring heat loses and 1 more in the heater). Finally, 6 thermocouples were also included in the insulation.

For the evaluation of thermal losses, some contact thermocouples are also distributed along the outer surface of the container and are located between the container shell and the external insulation (see Fig. 4).

Experiments were used to validate the finite element model developed, both considering static and dynamic analysis. The experiments carried out are:

- Isothermal tests: the electrical heater is switched on with given conditions and the tank is measured until all of it is at the same temperature. With this experiment the output to be evaluated is

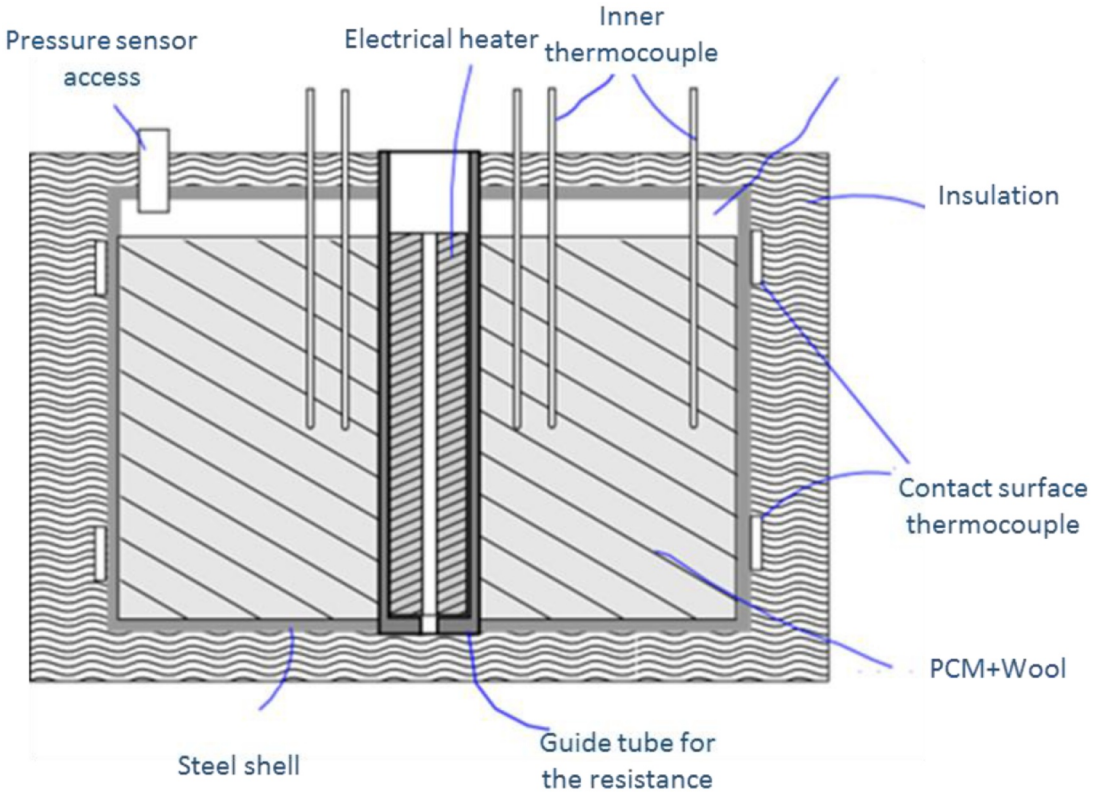

Fig. 1. Scheme of the experimental PCM tank.

effective thermal conductivity, thermal losses, and contact resistance.

- Dynamic cycling: melting and freezing cycles are carried out to evaluate the PCM performance.

3. Model description

The heat transfer flows in the PCM storage tank are presented in Fig. 5. The energy balance of the system is described by:

$$Q_{Res} = Q_{np} + Q_{in} \tag{1}$$

$$Q_{in} = Q_{Lat} + Q_{BOT} + Q_{TOP} \tag{2}$$

where Q_{Res} is the energy given by the electrical resistance, Q_{np} is the energy from the electrical resistance lost from its top and bottom, Q_{in} is the energy from the electrical resistance going into the PCM, Q_{Lat}, Q_{TOP}, and Q_{BOT} is the energy lost in the lateral, top, and bottom side of the container, respectively.

The storage tank is modelled considering discharging the composite (solidification) and charging it (melting) around a cylindrical pipe where the heat transfer fluid (HTF) flows inside and the composite is around it, following the model presented in Abujas et al. 2016. During solidification, the Stephan equation for cylinders is used, when a solid layer of PCM (salt) is formed around the pipe [12]:

$$t = \frac{H_{lat}\cdot\rho\cdot s^2}{2k(T_m - T_0)} f(s^+, \beta) \tag{3}$$

$$\beta_{cil} = \frac{k}{k_{wall}} \ln\left(\frac{R}{R - e_{wall}}\right) + \frac{k}{\alpha(R - e_{wall})} \tag{4}$$

$$f(s^+, \beta) = \left(1 + \frac{1}{s^+}\right)^2 \ln(1 + s^+) - \left(1 + \frac{2}{s^+}\right)\left(\frac{1}{2} - \beta\right) \tag{5}$$

$$s^+ = s/R \tag{6}$$

Where:

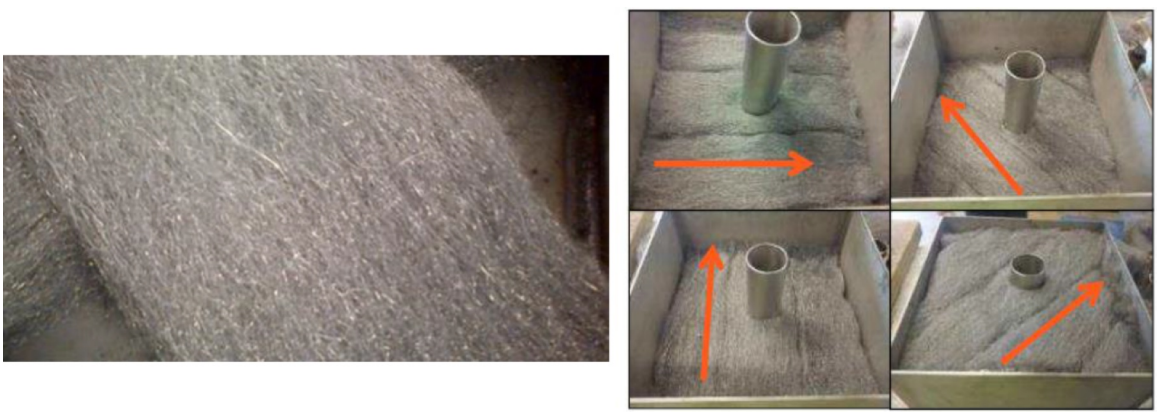

Fig. 2. Metal wool inserted in the storage tank.

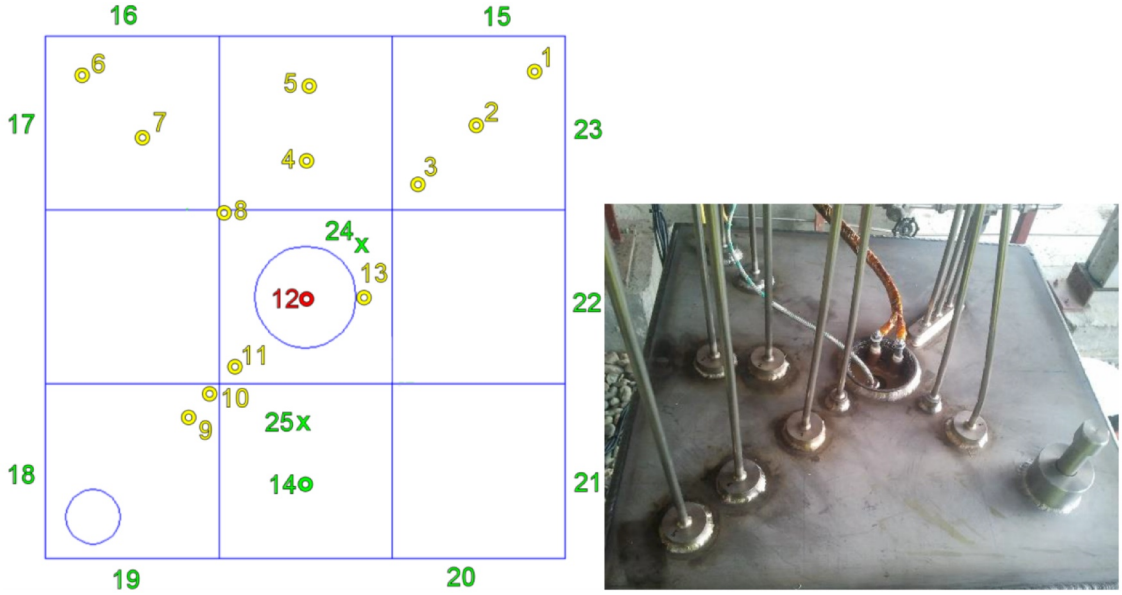

Fig. 3. Thermocouples distribution used in the storage tank.

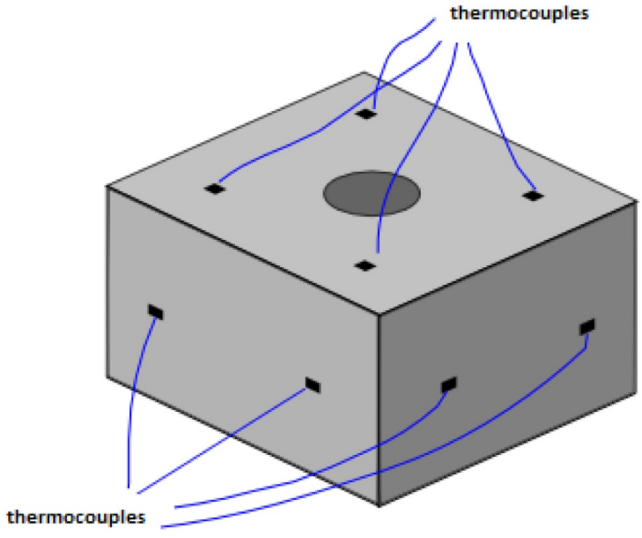

Fig. 4. Thermocouples distribution in the surface.

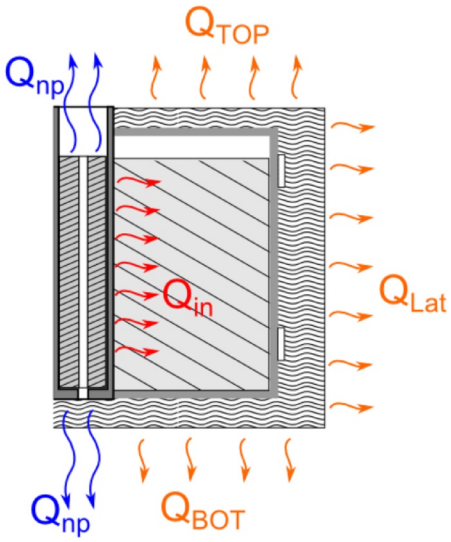

Fig. 5. Heat transfer flows in the PCM tank.

H_{lat}: PCM phase change entalphy
s: PCM layer thickness
k: PCM thermal conductivity
T_m: PCM melting temperature
T_0: Interior surface temperature
f: Cylinder factor
ρ: PCM density
s^+: Non-dimensional layer advance
β: Thermal resistance coefficient
k_{wall}: Interior tube conductivity
R: Interior radius
α: Heat transfer coefficient
e_{wall}: Wall thickness

The model consists of an axisymmetric cross-section, representing the flow of HTF through the pipe and the PCM that surrounds these pipes. In general, for a cylindrical domain with homogeneous, isotropic thermal conductivity, the enthalpy equation gives:

$$\frac{\partial h}{\partial t} = \frac{\kappa}{r}\left[\frac{\partial}{\partial r}\left(r\frac{\partial T}{\partial r}\right)\right] + \kappa\frac{\partial}{\partial z}\left(\frac{\partial T}{\partial z}\right) \tag{7}$$

On the other hand, our problem is not quite so simple. This simple equation does not apply near the wall since we have a pipe that has a different thermal conductivity from the composite. The pipes are considered by using an effective thermal conductivity for the composite element closest to the pipe, and the heat storage capacity of the pipes is not taken into account. The effective thermal conductivity is considered the maximum possible of the homogeneous mixture of two materials:

$$k_{eff}^{MAX} = \varepsilon k_{PCM} + (1-\varepsilon)k_{Wool} \tag{6a}$$

where:

ε: Volumetric proportion of the different compounds
k: Composite thermal conductivity

A 2D model was developed, generating two symmetry planes. Each layer was represented by four surfaces, representing the storage material, the container material and the two insulation layers (Fig. 6). The

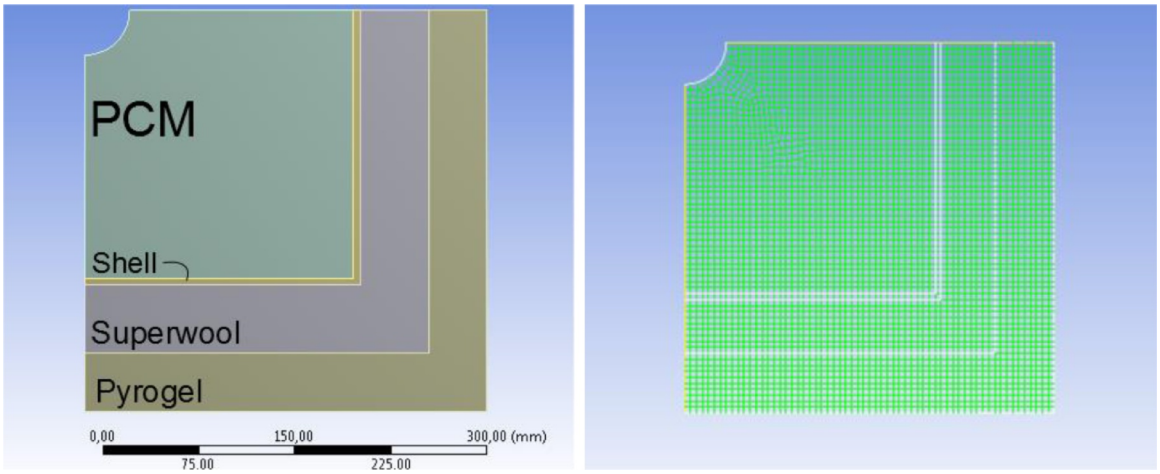

Fig. 6. Layers used in the modelling of the storage tank.

model was discretized with a uniform mesh of about 5 mm what means 3808 elements in the model with a time step of 0,05 s. A grid refinement study of the mesh was carried out, reducing the time step to avoid divergence and optimising Δr, being Δr the most important factor for precision.

The considered boundary conditions were an ambient temperature of 10 ˚C.

At wall, radial heat transfer with convection and conduction through wall thickness is considered.

At all points along the tube axis, the fluid characteristics (temperature, enthalpy, and quality) are calculated at each time iteration. These fluid properties allow calculation of the rest of the fluid properties, such as Prandtl number and viscosity.

First a stationary analysis was carried out with the aim of evaluating the temperature distribution in the storage tank. The study was carried out at 190 ˚C, 250 ˚C, and 290 ˚C. The effective thermal conductivity of the insulation materials was found with this evaluation as detailed above.

4. Model validation

As first approximation, the temperature distribution inside the tank in steady state conditions is modelled. The same temperatures as those tested experimentally were modelled, 190 ˚C, 250 ˚C, and 290 ˚C.

The effective thermal conductivity of the composite was calculated with a parametric study of the heat losses of the tank, using a penalization to the thermal conductivity, K_{pen}. Results for 250 ˚C were the following, with the simulation and its comparison with the experimental results presented in Fig. 7:

$$K_{pen} = 3.8\,k_{mat} = 1.99\,W/mK$$
$$\overline{\Delta T} = 2.\ 25°C\ \ \Delta T_{MAX} = 6°C\ \ \Delta T_{min} = 0.\ 48°C$$
$$\dot{Q}_h^{SIM} = 73.95\,W\ \ \dot{Q}_h^{EXP} = 73.47\,W$$

where:

k_{mat}: Composite thermal conductivity (W/mK)
ΔT: Difference between experimental and simulated temperature (˚C)
Q: Heat in the system (W)

Similarly, results for the case of 150 ˚C are shown in F *Fig. 8* and those for 290 in Fig. 9. From these experiments, the final effective thermal conductivity of the composite is considered to be 2 W/m•K, which is 300% higher than that of the pure salt.

The analysis of the static points has made possible to determine the operating conditions related to the insulation and the effective conductivity of the material. To determine if the thermal inertia values are adequate, the transition states between static points are analysed, keeping constant the rest of the values. The results are shown Fig. 10 and Fig. 11, where the solid lines reflect the values obtained experimentally and the dashed lines reflect the values obtained in the simulation. e. shows the comparison between experimental results and simulation. Results showed good adjustment of results

It is considered that the trend of the model corresponds to the results obtained experimentally, which confirms that the model is valid for the study of analysis of transients in the prototype.

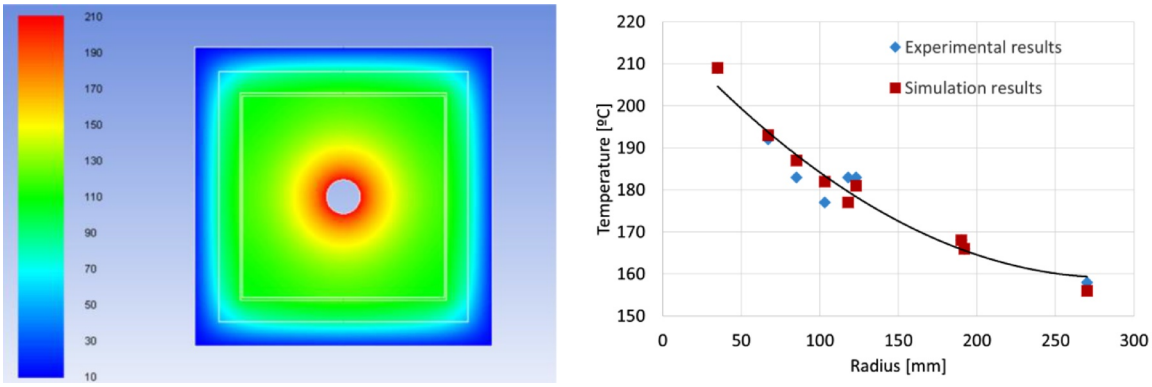

Fig. 7. Left: simulation of the temperature (˚C) distribution for the 250 ˚C case. Right: comparison with experimental results.

$\overline{\Delta T} = 2.59ºC$

$\Delta T_{MAX} = 4.37ºC$

$\Delta T_{min} = 0.23ºC$

$\dot{Q}_h^{SIM} = 39.79\ W$

$\dot{Q}_h^{EXP} = 37.54\ W$

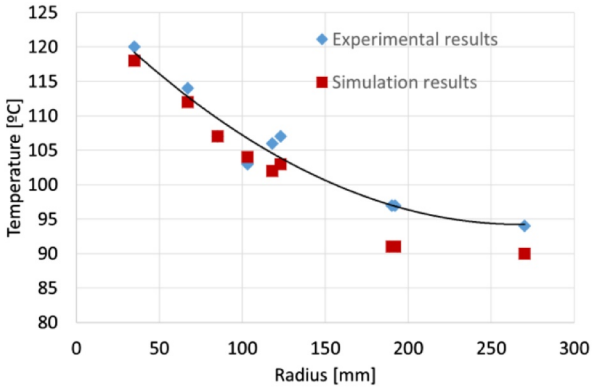

Fig. 8. Results for the 190 °C case.

5. Results

5.1. Dynamic cycling of pcm

To model the dynamic behaviour of the composite, first only conduction heat transfer is used. The simulation of the melting/solidification process is carried out maintaining the same configuration already explained. The comparison with the experimental PCM melting results are shown in Fig. 12. As it can see, the results obtained by the simulation (dashed lines) do not correspond to the results obtained experimentally (solid line). It can be seen that the result once the steady state is reached is very different for each case.

The Fig. 13 shows how the distribution of temperature (left) and internal energy (right) of the simulation are not consistent when the model considers just the conduction as the main transport mechanism. In this simulation, only the PCM next to the pipe changes phase (high internal energy area), while in the experiments all the PCM has melted. This implies that the convection phenomenon is not negligible for this application, there is a movement within the molten material that allows the temperature to be uniformized therein. [8,13]. To include this phenomenon of uniformization without having to resolve the movement of the fluid, a high conductivity is artificially introduced. Differenthigh thermal conductivity values where used, 20 W/m•K, 200 W/m•K, and 2000 W/m•K, finding the best results with 20 W/m•K (Fig. 14), where the experimental (dashed lines) and simulation (solid lines) results of the PCM melting when a thermal conductivity of 20 W/m•K is considered has significantly improved their approach. The whole system is melted and there is no appreciable temperature gradient on the final state.

The simulation of the freezing case is carried out next. The internal resistance is shutdown. There is a slow cooling that allows distinguishing the freezing of the different layers. The comparison with experimental results is presented in Fig. 15. The simulation results show a slower freezing than the experimental ones. Minimal temperature variations imply significant changes in the energy contained in the material close to the phase change.

A heat flux boundary condition is defined in the electric resistance, the agreement reached is adequate (Fig. 16) and the temperature distribution is more aligned with the expected one (Fig. 17).

5.2. Comparison of thermal conductivity enhancement techniques

The theoretical comparison was carried out considering a cylindrical pipe with 24 mm of diameter at 307 °C initial temperature, being melted with the HTF. The stored energy and melting displacement results of the $NaNO_3$ as PCM alone are presented in *Fig. 18*. After 8 h of heating, the PCM is melted up to 47 mm diameter, storing around 0.12 kWh/m, giving an average power of 0.3 kW, which is in accordance with the values found in the literature [14,15].

As stated before, when fins are added to the PCM, the thermal conductivity increases [6]. The fin system studied by DLR [16] and Abengoa [6] was modelled (*Fig. 19*), considering the properties shown in *Table 5*. The obtained results are shown in *Fig. 20*. In this configuration, when fins are used, the energy stored and the melting velocity increase. After 8 h already 34% of the PCM melts, storing around 0.3 kWh/m with an average power of 0.75 kW.

The effect of metal wool as thermal conductivity enhancement technique was studied with the characteristics shown in Table 3, Table 6 and Table 7, and the results are presented in *Fig. 21*. In this configuration, when wools and $NaNO_3$ are used as PCM composite, the energy stored and the melting velocity present the highest value. After 8 h of melting, the stored energy is 0.72 kWh/m with an average power of 1.23 kW. Comparing these results with the results of the configuration with 10% fins of the same material gives a storage power of 64% greater (1.23 kW vs. 0.75 kW).

$\overline{\Delta T} = 4.7ºC$

$\Delta T_{MAX} = 8ºC$

$\Delta T_{min} = 1.16ºC$

$\dot{Q}_h^{SIM} = 90.31\ W$

$\dot{Q}_h^{EXP} = 87.40\ W$

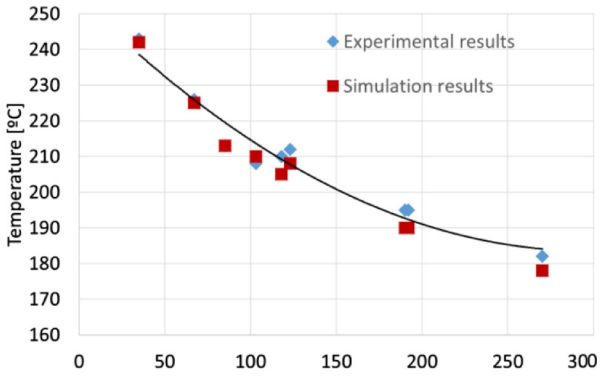

Fig. 9. Results for the 290 °C case.

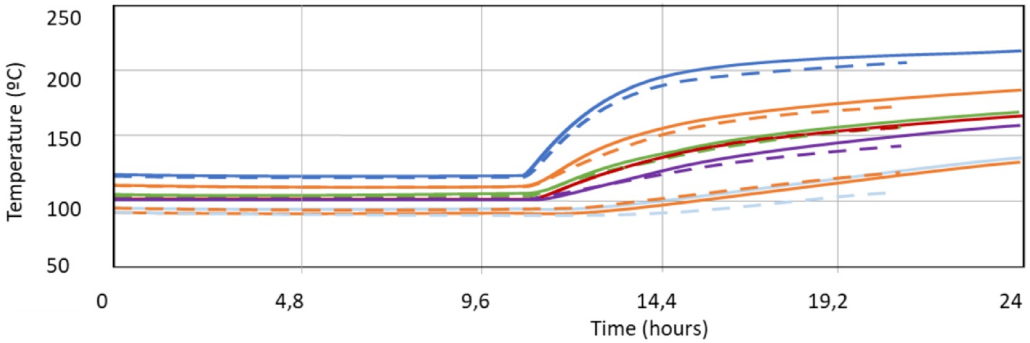

Fig. 10. Experimental (dashed lines) and simulation (solid lines) results of the PCM heating up between 150 °C and 250 °C.

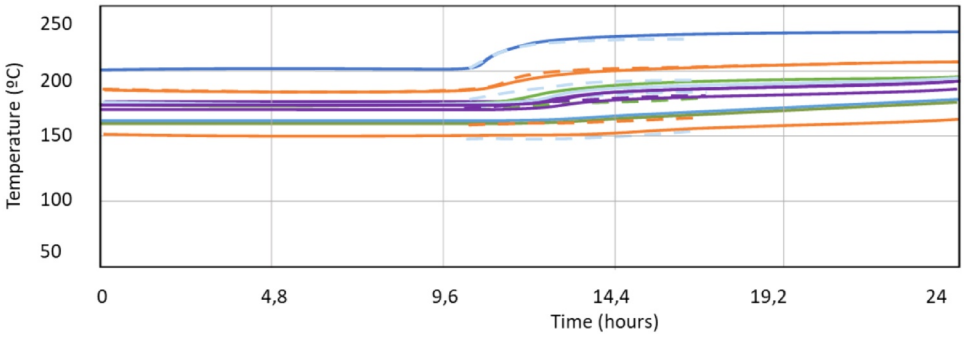

Fig. 11. Experimental (dashed lines) and simulation (solid lines) results of the PCM heating up between 250 °C and 290 °C.

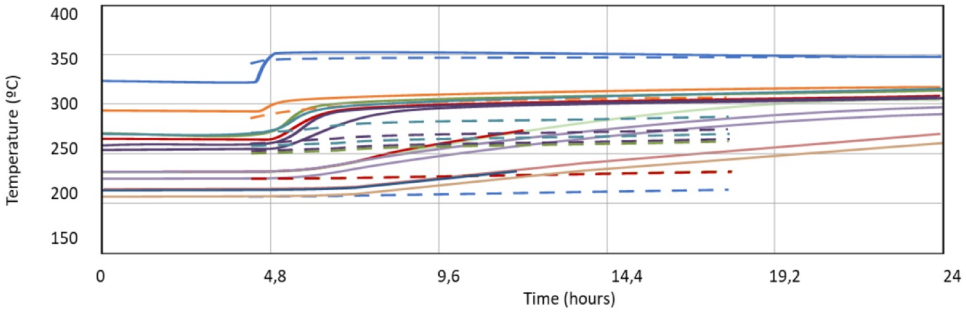

Fig. 12. Experimental (dashed lines) and simulation (solid lines) results of the PCM melting when only conduction heat transfer is considered.

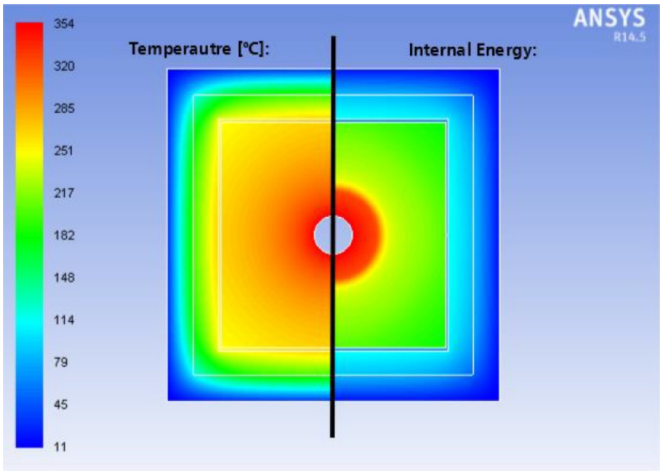

Fig. 13. Simulation of the PCM behaviour when only conduction heat transfer is considered. Left: temperature distribution; right: internal energy distribution.

6. Conclusions

This paper addresses one important barrier for the deployment of the use of phase change materials, their low thermal conductivity. To overcome this disadvantage, a simple, cheap, and often disregarded method is thoughtfully investigated, the use of metal wool.

Results show that using metal wool with the appropriate porosity and arrangement can increase significantly the effective thermal conductivity of a composite storage tank without decreasing the energy density to unacceptable values, which was one of the main problems found in former studies. The temperature of the PCM used ($NaNO_3$) shows that this would be a good solution for industrial applications, both of solar energy use or of waste heat reuse.

A storage finite element model is developed and is validated experimentally in a prototype. Static analysis, dynamics, and finally phase change analysis (fusion and crystallization) are implemented in the model validation.

The static tests in solid state have shown an effective conductivity of 2 W/m•K in the composite, that means an increase of 300% in comparison with the salt conductivity. The tests carried out during the melting process have determined that the movement of the fluid standardizes the temperature of the molten material. Different tests were

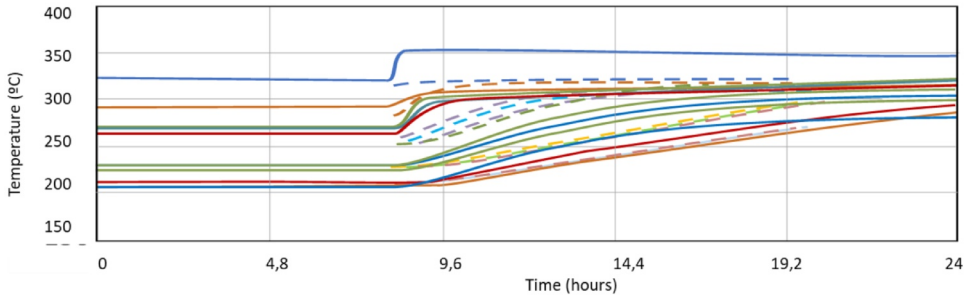

Fig. 14. Experimental (dashed lines) and simulation (solid lines) results of the PCM melting when a thermal conductivity of 20 W/m•K is considered.

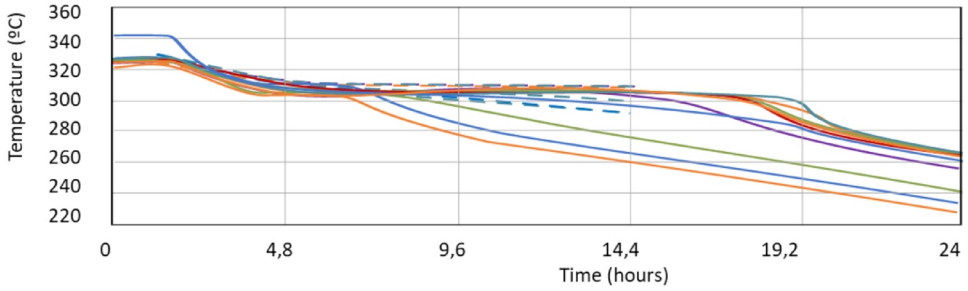

Fig. 15. Experimental (dashed lines) and simulation (solid lines) results of the PCM freezing when a thermal conductivity of 20 W/m•K is considered.

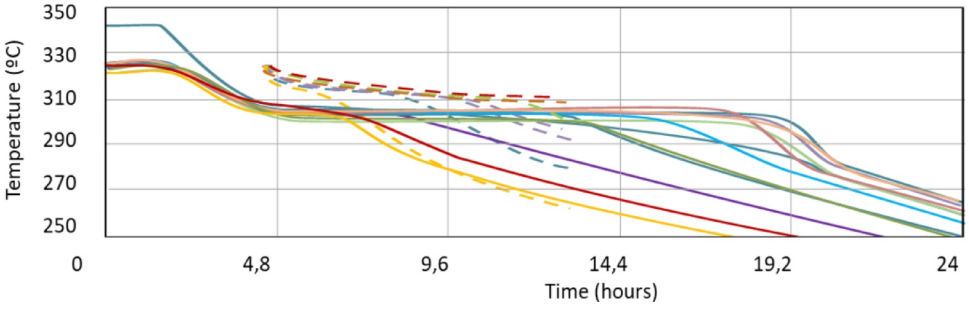

Fig. 16. Experimental (dashed lines) and simulation (solid lines) results of the PCM freezing when a thermal conductivity of 20 W/m•K and heat flux boundary conditions are considered.

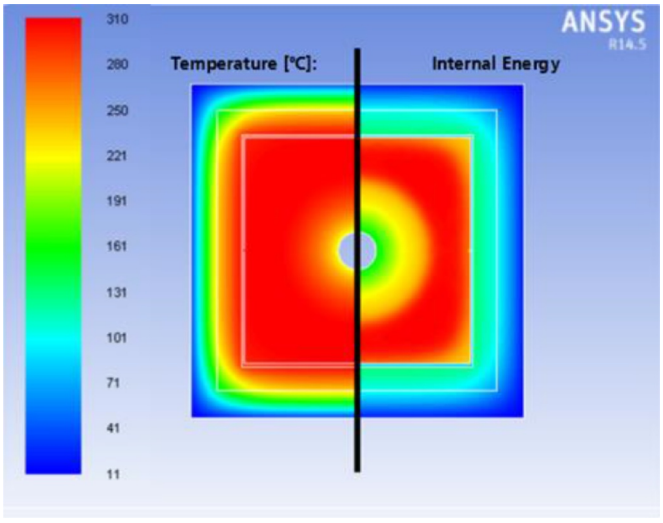

Fig. 17. Simulation of the PCM behaviour when convection heat transfer with heat flux boundary conditions is considered. Left: temperature distribution; right: internal energy distribution.

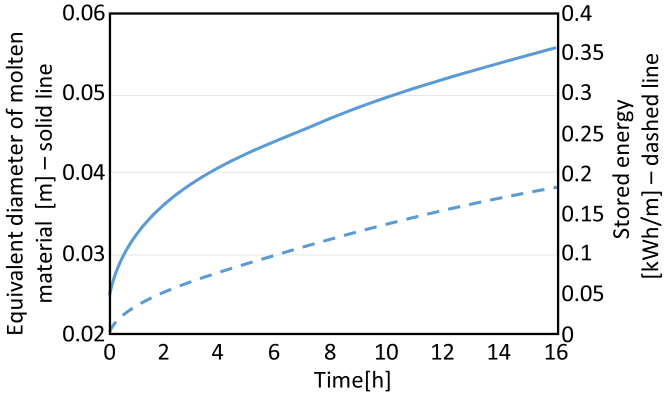

Fig. 18. Stored energy in the Na NO3 as PCM and melting diameter displacement.

carried out to quantify this effect and finally determining that the composite behaves as if there is a conductivity in the liquid zone equal to 20 W/m•K. The system was successfully characterized. The main mechanisms of energy transfer were detected, and the new model can be used for the dimensioning of the heat storage applications.

A comparison with the use of fins in the PCM, a more common method of thermal conductivity enhancement, has also shown that the

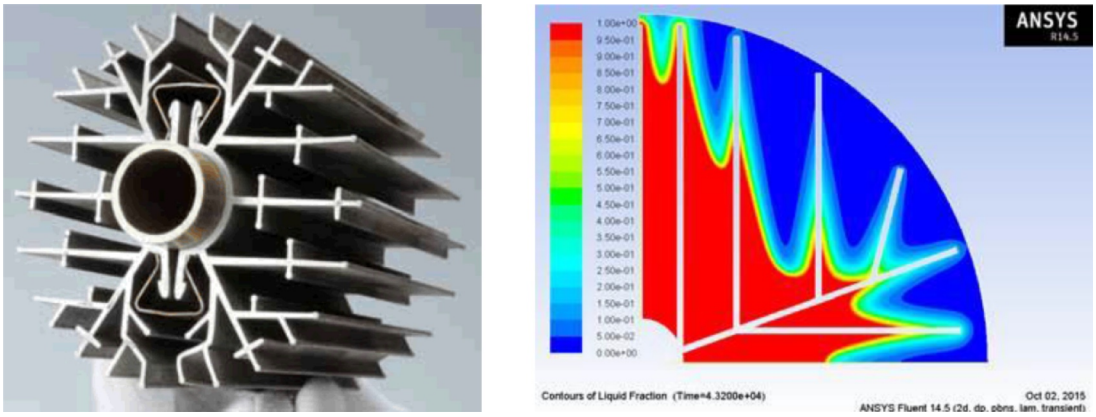

Fig. 19. Left: Fins studied. Right: Simulation of the system.

Table 5
Characteristics of the fin system added to the PCM.

Characteristic / Property	Value
Material	Carbon steel
Thermal conductivity	40 W/m•K
Density	8030 kg/m3
Specific heat	0.502 kJ/kg•K
External pipe diameter	0.024 m
Pipe thickness	0.002 m
PCM total diameter	0.120 m
Fins thickness	0.001 m
Fins area in the PCM	10%

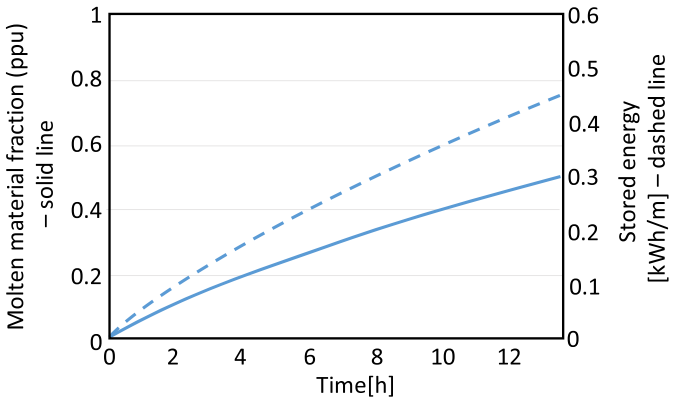

Fig. 20. Stored energy in the Na NO3 with fins as PCM composite and melting diameter displacement.

Table 6
Characteristics of the metal wool.

Characteristic / Property	Value
Material	Steel metal wool
Porosity	90%
Thermal conductivity	40 W/m•K

Table 7
Characteristics of the composite PCM + wool.

Characteristic / Property	Value
Density of PCM composite	2495 kg/m^3
Effective thermal conductivity	4.48 W/m•K
Energy density	12 kJ/kg

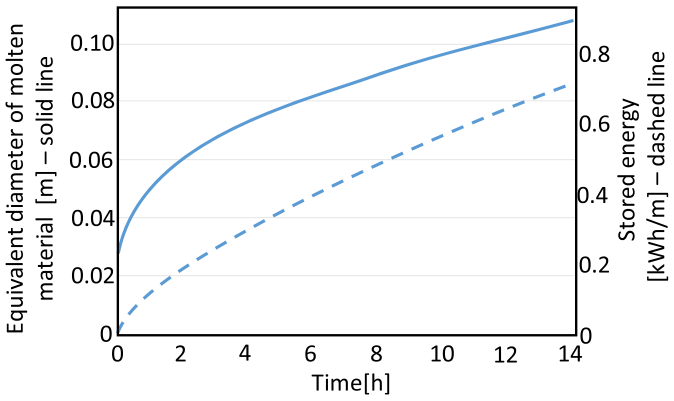

Fig. 21. Stored energy in the Na NO3 with wools as PCM composite and melting diameter displacement.

steel wool composite model, with the addition of the same amount of material (10% volume in both cases) and a simpler assembly process to the fin assembly, has significantly improved the heat transfer.

CRediT authorship contribution statement

Cristina Prieto: Conceptualization, Methodology, Validation, Writing - review & editing. **Carlos Rubio:** Software, Validation. **Luisa F. Cabeza:** Writing - review & editing.

Declaration of Competing Interest

The authors declare that they have no known competing financial interests or personal relationships that could have appeared to influence the work reported in this paper.

Acknowledgements

The research leading to these results has received funding from CDTI in the project Innterconecta Thesto (ITC-20111050). The work partially funded by the by the Ministerio de Ciencia, Innovación y Universidades de España (RTI2018–093849-B-C31 - MCIU/AEI/FEDER, UE). This work was partially funded by the Ministerio de Ciencia, Innovación y Universidades - Agencia Estatal de Investigación (AEI) (RED2018–102431-T). Dr. Cabeza would like to thank the Catalan Government for the quality accreditation given to her research group GREiA (2017 SGR 1537). GREiA is certified agent TECNIO in the category of technology developers from the Government of Catalonia. This work is partially supported by ICREA under the ICREA Academia programme.

Supplementary materials

Supplementary material associated with this article can be found, in the online version, at doi:10.1016/j.est.2020.101926.

References

[1] M.H. Abokersh, M. Osman, O. El-Baz, M. El-Morsi, O. Sharaf, Review of the phase change material (PCM) usage for solar domestic water heating systems (SDWHS), Int. J. Energy Res. 42 (2018) 329–357, https://doi.org/10.1002/er.3765.

[2] S.Y. Kee, Y. Munusamy, K.S. Ong, Review of solar water heaters incorporating solid-liquid organic phase change materials as thermal storage, Appl. Therm. Eng. 131 (2018) 455–471, https://doi.org/10.1016/j.applthermaleng.2017.12.032.

[3] A.K. Pandey, M.S. Hossain, V.V. Tyagi, N. Abd Rahim, J.A.L. Selvaraj, A. Sari, Novel approaches and recent developments on potential applications of phase change materials in solar energy, Renew. Sustain. Energy Rev. 82 (2018) 281–323, https://doi.org/10.1016/j.rser.2017.09.043.

[4] C. Prieto, L.F. Cabeza, Thermal energy storage (TES) with phase change materials (PCM) in solar power plants (CSP). Concept and plant performance, Appl. Energy. 254 (2019) 113646, , https://doi.org/10.1016/j.apenergy.2019.113646.

[5] J. Gasia, L. Miró, L.F. Cabeza, Materials and system requirements of high temperature thermal energy storage systems: a review. Part 2: thermal conductivity enhancement techniques, Renew. Sustain. Energy Rev. 60 (2016), pp. 1584–1601, https://doi.org/10.1016/j.rser.2016.03.019.

[6] C. Rubio Abujas, A. Jové, C. Prieto, M. Gallas, L.F. Cabeza, Performance comparison of a group of thermal conductivity enhancement methodology in phase change material for thermal storage application, Renew. Energy. 97 (2016) 434–443, https://doi.org/10.1016/j.renene.2016.06.003.

[7] H. Badenhorst, A review of the application of carbon materials in solar thermal energy storage, Sol. Energy. 192 (2019) 35–68, https://doi.org/10.1016/j.solener.2018.01.062.

[8] J.M. Mahdi, E.C. Nsofor, Multiple-segment metal foam application in the shell-and-tube PCM thermal energy storage system, J. Energy Storage. 20 (2018) 529–541, https://doi.org/10.1016/j.est.2018.09.021.

[9] J. Gasia, J.M. Maldonado, F. Galati, M. De Simone, L.F. Cabeza, Experimental evaluation of the use of fins and metal wool as heat transfer enhancement techniques in a latent heat thermal energy storage system, Energy Convers. Manag. 184 (2019) 530–538, https://doi.org/10.1016/j.enconman.2019.01.085.

[10] M.S. Yousef, H. Hassan, An experimental work on the performance of single slope solar still incorporated with latent heat storage system in hot climate conditions, J. Clean. Prod. 209 (2019) 1396–1410, https://doi.org/10.1016/j.jclepro.2018.11.120.

[11] M.S. Yousef, H. Hassan, Energetic and exergetic performance assessment of the inclusion of phase change materials (PCM) in a solar distillation system, Energy Convers. Manag. 179 (2019) 349–361, https://doi.org/10.1016/j.enconman.2018.10.078.

[12] S. Jegadheeswaran, S.D. Pohekar, Performance enhancement in latent heat thermal storage system: a review, Renew. Sustain. Energy Rev. 13 (2009) 2225–2244, https://doi.org/10.1016/j.rser.2009.06.024.

[13] R.E. Murray, D. Groulx, Experimental study of the phase change and energy characteristics inside a cylindrical latent heat energy storage system: part 1 consecutive charging and discharging, Renew. Energy. 62 (2014) 571–581, https://doi.org/10.1016/j.renene.2013.08.007.

[14] H.A. Zondag, R. de Boer, S.F. Smeding, J. van der Kamp, Performance analysis of industrial PCM heat storage lab prototype, J. Energy Storage. 18 (2018) 402–413, https://doi.org/10.1016/j.est.2018.05.007.

[15] C. Li, Q. Li, Y. Ding, Investigation on the thermal performance of a high temperature packed bed thermal energy storage system containing carbonate salt based composite phase change materials, Appl. Energy. 247 (2019) 374–388, https://doi.org/10.1016/j.apenergy.2019.04.031.

[16] M. Christ, O. Ottinger, W.D. Steinmann, Latent heat storage devices, US2007/0175609A1, 2007.